Online Appendix for "Information Matters: Feasible Policies for Reducing Methane Emissions"

Karl Dunkle Werner and Wenfeng Qiu

August 21, 2024

A1 Proofs and Technical Details

A1.1 Proof of Proposition 1

Proof: Because C_i' is strictly increasing and convex, $C_i'^{-1}(x) =: f(x)$ is strictly increasing and concave.

$$\frac{\partial \text{DWL}_i}{\partial t_i} = -\frac{\partial C_i'^{-1}(e_i \cdot (p_i + t_i))}{\partial t_i} \cdot e_i(\delta - t_i) = -f' \cdot e_i^2(\delta - t_i) < 0$$

$$\frac{\partial^2 \text{DWL}_i}{\partial t_i^2} = -\frac{\partial f' \cdot e_i^2(\delta - t_i)}{\partial t_i} = -e_i^2(\underbrace{f'' \cdot e_i(\delta - t_i)}_{<0} - f') > 0$$

□

A1.2 Proof of Proposition 2

Proof: The feasible set under the constraint is a compact subset of $\mathbb{R}^N$ so a solution exists. Because DWL_i only depends on r_i and DWL_i is strictly increasing, convex in r_i and the constraints are linear inequalities, we conclude a unique solution exists and can be characterized by the standard Karush–Kuhn–Tucker (KKT) conditions.

Let r_i^*s be the solution of the problem. Suppose there exists k, j such that $e_k > e_j$ but $r_k^* < r_j^*$. Consider $\hat{r}_i$s such that $\hat{r}_i = r_i^*$ for all $i \neq k, j$ and $\hat{r}_k = r_j^*, \hat{r}_j = r_k^*$. Clearly, r_i^* also satisfy all the constraints. The difference in the total DWL for $\hat{r}_i$s and r_i^*s is equal to

$$
\begin{aligned}
&\mathrm{DWL}_k(\hat{r_k}) + \mathrm{DWL}_j(\hat{r_j}) - (\mathrm{DWL}_k(r_k^*) + \mathrm{DWL}_j(r_j^*)) \\
=&\mathrm{DWL}_k(r_j^*) - \mathrm{DWL}_k(r_k^*) + \mathrm{DWL}_j(r_k^*) - \mathrm{DWL}_j(r_j^*) \\
=&\int_{r_k^*}^{r_j^*} \frac{\partial \mathrm{DWL}_k}{\partial r_k}\, dr + \int_{r_j^*}^{r_k^*} \frac{\partial \mathrm{DWL}_j}{\partial r_j}\, dr \\
=&\int_{r_k^*}^{r_j^*} \frac{\partial \mathrm{DWL}_k}{\partial r_k} - \frac{\partial \mathrm{DWL}_j}{\partial r_j}\, dr
\end{aligned}
$$

Since $\frac{\partial^2 \mathrm{DWL}_i}{\partial r_i \partial e_i} < 0$ and $e_k > e_j$, the integrand is negative and hence the whole integral is negative, which implies DWL under $\hat{r_i}$s is small. This a contradiction to r_i^*s being optimal. □

Note that for the estimation part, the inequality $\frac{\partial^2 \mathrm{DWL}_i}{\partial r_i \partial e_i} < 0$ follows directly from the specific choice function we chose and the expected fee t_i being an increasing function of r_i,

$$
\frac{\partial^2 DWL_i}{\partial t_i \partial e_i} = \left(1 + \frac{1}{\alpha}\right) e_i^{\frac{1}{\alpha}} \frac{(\delta - t_i)}{\alpha(p_i + t_i)} \left(\frac{(p_i + t_i)}{A}\right)^{\frac{1}{\alpha}} < 0
$$

A1.3 Proof of Proposition 3

Proof: Suppose there is no leak observed for a well. Then the well operator will not pay any fee even when the well pad is audited because the leak detection threshold is the same for remote measurement and the audit under Policy 3a. It follows that the regulator should not audit this well pad to save the audit budget.

Let r_i^*s be the optimal audit probabilities for Policy 2 so $\sum_{i=1}^N r_i^* \leq M$. Because $0 \leq q_i \leq 1$, $\sum_{i=1}^N \Big(q_i \cdot 0 + (1 - q_i) r_i^*\Big) \leq M$. That is, every set of feasible audit probabilities r_i^*s for Policy 2 is also feasible for Policy 3a. Since Policy 2 has the same objective function as Policy 3a, it follows the regulator achieves a higher DWL reduction. □

A1.4 Extensive form game trees for policies 2 and 3a

Figure A1: Game tree: targeting on covariates (policy 2)

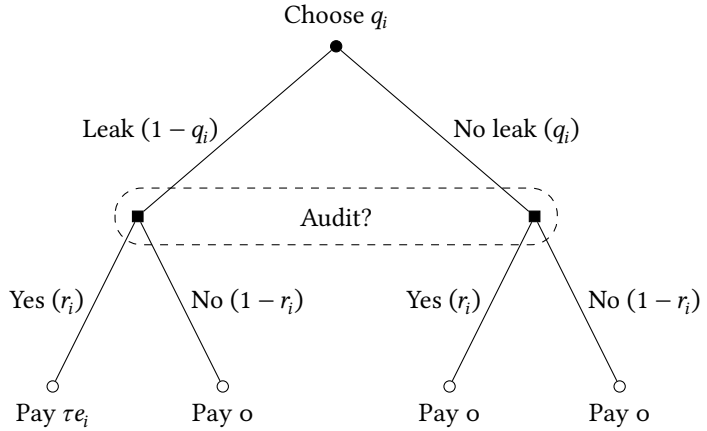

In this figure, the well operator chooses the probability of not having a leak, q_i, with full knowledge of the probability they will be audited, r_i. Then nature determines whether a leak occurs. The regulator does not know whether a leak has occurred—their information set is indicated in a dashed oval. If the well pad is leaking and is audited, the well operator pays τe_i. In all other cases, they pay zero.

Figure A2: Game tree: target leaks with no additional censoring (policy 3a)

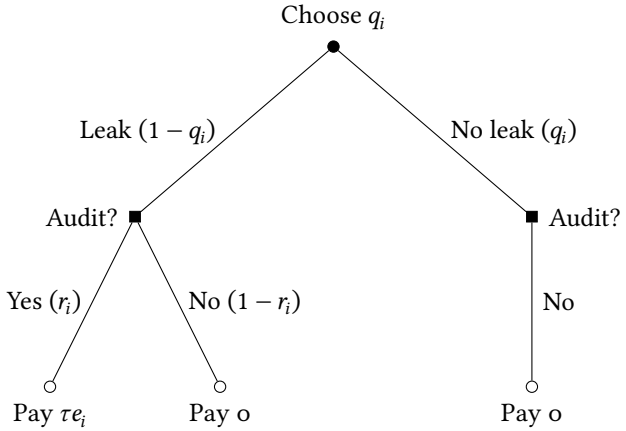

In this figure, the well operator chooses the probability of not having a leak, q_i, with full knowledge of the probability they will be audited, r_i. Then nature determines whether a leak occurs. The regulator knows when a leak has occurred, and will never audit a well pad that isn't leaking. If the well pad is leaking and is audited, the well operator pays τe_i. In all other cases, they pay zero.

A1.5 Policy 3b: Target auditing on observed emissions: high threshold

Policy 3b is the case where the regulator may observe very large leaks, over some detection threshold, then must decide which wells to audit. Only wells that are audited and leaking are assessed a fee. This policy is a generalization of policy 3a, which was the same but without a significant detection threshold.

Figure A3 has a game tree for the regulator's problem. Each well operator knows whether they're on the left branch (large e_i) or right branch (small e_i), since e_i is not a choice variable. The dashed oval indicates the regulator's information set—they cannot tell whether a well pad has a large e_i and isn't leaking, a small e_i and isn't leaking, or a small e_i and is leaking.

Figure A3: Game tree: target leaks (policy 3b) with censoring

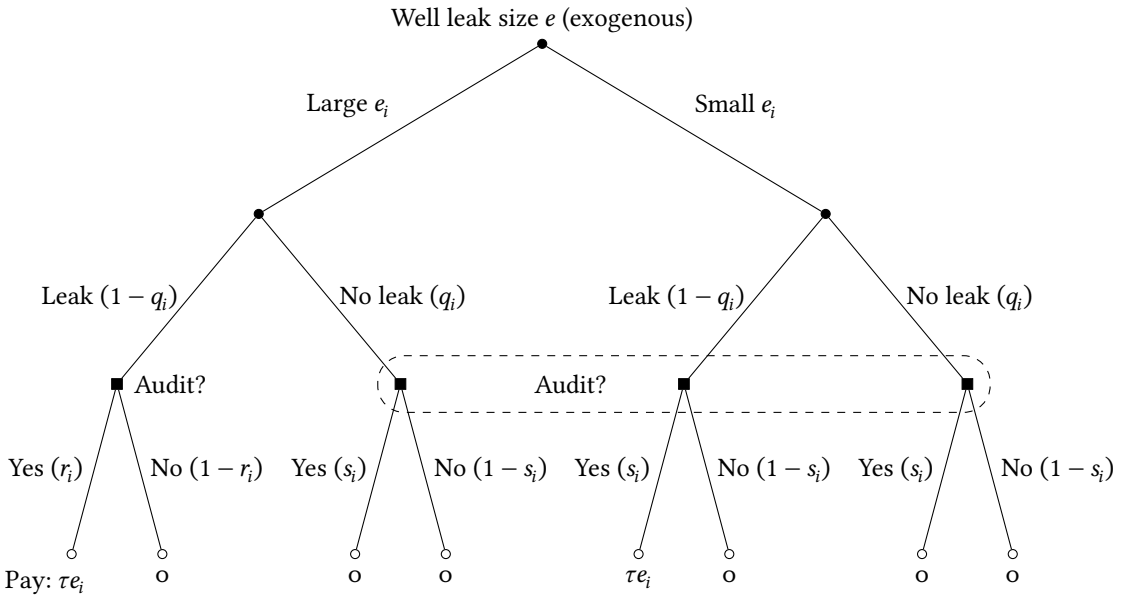

In this figure, nature determines the well's potential leak size, e_i. It is not a choice variable. The well operator knows e_i; the regulator can only form expectations. The well operator chooses their probability of not having a leak, q_i. If a leak happens at a large well, it is detected. If a leak happens at a small well, it is not. If a leaking well pad is audited, it pays τe_i. The dashed oval indicates the regulator's information set.

The regulator sets audit probabilities based on whether the leakage is detected,

taking the detection threshold into account. As the game tree suggests, if a well pad is *not* detected with leakage, there is no way to distinguish between whether it is actually not leaking or the leakage is small. As a result, the regulator can only specify an audit probability $r_i(X_i)$ for a well pad i with detected leakage and an audit probability $s_i(X_i)$ for a well pad with *no* detected leakage (the covariates X included in the brackets means the r, s can depend on these covariates).

A well operator's response to this policy will depend on their e_i. For small-e wells, their response is straightforward; because they know they will always be audited with probability s_i, the DWL will be $\text{DWL}_i(s_i)$. But for large wells, the incentives are more complicated. A large well pad i will have q_i probability of *not* leaking. But even when it is not leaking, it will be audited with probability $s_i(X_i)$. Since it is not leaking, the audit will not lead to any penalty (the auditing effort is wasted here). Large-e wells will not care about s_i. q_i and DWL_i will be functions that depend only on r_i. The *ex-ante* DWL for a large-e well pad will be $\text{DWL}_i(r_i)$.

The budget is similar to the case with no detection threshold. As with the DWL, it's the probability of being audited *when leaking* that matters to the well operator, so the large-e wells choose $q_i(r_i)$ (s_i does not enter). Unlike the previous cases, large-e wells now have some s_i probability of being audited when not leaking. Therefore, the audit costs are $(1-q_i(r_i))r_i + q_i(r_i)s_i$ for each large-e well, and s_i for each small-e well.

Given these DWL and budget components, the regulator needs to pick r_i and s_i. The regulator still does not know which wells are large-e or small-e, so optimizes a weighted average, where the weights are the probability the well's leak is above the threshold. For a detection threshold $\underline{e}$, define $z_i \equiv \Pr(e > \underline{e} \mid X_i)$. The regulator then optimizes the problem:

$$\begin{aligned} \min_{\{r_i\}_{i=1}^N, \{s_i\}_{i=1}^N} \quad & \sum_i z_i \text{DWL}_i(r_i) + (1-z_i)\text{DWL}_i(s_i) \\ & s.t. \ \sum_i z_i[(1-q_i(r_i))r_i + q_i(r_i)s_i] + (1-z_i)s_i \leq M \\ & \forall i \ : \ r_i \in [0,1], s_i \in [0,1] \end{aligned}$$

We can compare this minimization problem with the previous one, where $\underline{e} = 0$, to

confirm that the previous problem was a special case of this one. In the previous problem, z_i converges to 1, so we do not need to worry about s_i in the objective function. Moreover, in the budget constraint, s_i should be set to zero to save audit effort. Lowering the detection threshold leads to a lower DWL.

A2 Methane Measurement

Figure A4: Production segment is responsible for 58% of leaks from natural gas supply chain

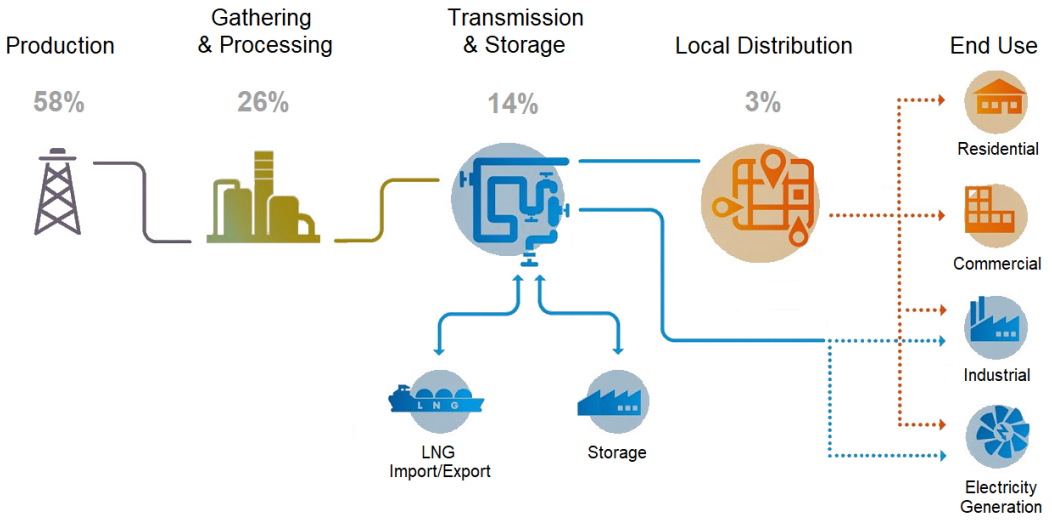

SOURCE: Marks (2022) figure 1, from estimates in Alvarez et al. (2018). Excludes end-use leaks.

Table A1: Estimated satellite detection varies by leak size and background

Surface type	True emissions (kg/hr)	Estimated emissions (kg/hr)
Grass	100	No detection
Grass	500	279 (101)
Grass	900	542 (38)
Bright	100	93.5 (18.3)
Bright	500	338 (83.1)
Bright	900	577 (115)

Note: Table is a subset of Cusworth et al. (2019) table 2 (CC BY 4.0). Results simulate methane retrievals from the EnMAP satellite, expected to launch in 2021. Values in parentheses are standard deviations from five iterations. We exclude the paper's results for images with "dark" or "urban" backgrounds, as these include water and confuse the image processing algorithm. In personal communication, the lead author notes "one could dramatically improve the prediction if there were some sort of decision tree that was based on the underlying surface."

Figure A5: Distribution of detected methane leaks, comparison with ground-based measurement

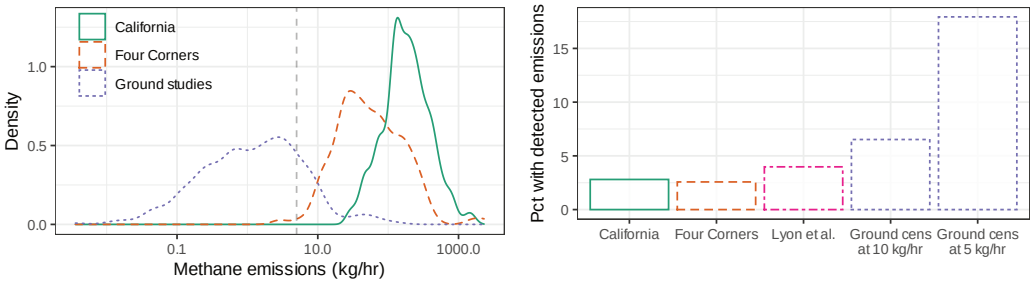

LEFT: emissions conditional on detection. RIGHT: fraction of well pads with detected emissions. The "ground cens at" columns are the ground studies' observations with artificial censoring applied, at either 5 or 10 kg/hr, the approximate detection threshold of both the California and Four Corners studies. Without artificial censoring, the ground-based measurements are non-zero approximately 97% of the time. 5 kg/hr is noted with a dashed line in the left plot.

SOURCES: Ground studies include measurements primarily from Robertson et al. (2017) with additional contributions from Rella et al. (2015), Omara et al. (2016), and Omara et al. (2018).

California and Four Corners distributions come from aircraft studies (Duren et al. 2019; Frankenberg et al. 2016). Lyon et al. (2016) provides information about leak prevalence (with a detection threshold roughly similar to the California and Four Corners studies), but not leak size.

Table A2: Balance comparison: well pads with and without detected leaks differ, but with overlapping covariate support

	California		Four Corners		Lyon et al. (2016)	
	Detect	No detect	Detect	No detect	Detect	No detect
Age (yr)	19.2	16.8	18.3	19.6	4.12	9.66
	[2.4,40]	[2.8,40]	[6.6,28]	[7.1,37]	[0.42,8.8]	[1.9,23]
Gas (mcfd)	282	88.7	326	153	1510	339
	[0.41,160]	[0.35,130]	[47,760]	[23,350]	[11,2800]	[2,610]
Oil (bbld)	142	25.8	0.103	0.233	300	37.5
	[0.9,70]	[0.98,43]	[0,0.14]	[0,0.53]	[0,880]	[0,59]
Detect leak (%)	100	0	100	0	100	0
	[100,100]	[0,0]	[100,100]	[0,0]	[100,100]	[0,0]
Gas price ($/mcf)	2.91	2.93	2.56	2.56	3.94	3.72
	[2.9,3]	[2.9,3]	[2.6,2.6]	[2.6,2.6]	[3.9,4.2]	[2.5,4.3]
Dist. to next pad (km)	0.114	0.0884	0.499	0.362		
	[0.051,0.18]	[0.048,0.15]	[0.21,0.74]	[0.14,0.63]		
N wells within 10 km	10100	10900	951	1240		
	[2000,18000]	[3700,25000]	[540,1300]	[780,1700]		

Note: Values are means, with the 10th to 90th percentile value in brackets. California and Four Corners data are from the "next generation airborne visible/infrared imaging spectrometer" (AVIRIS-NG) sample (panel A of table 1). Lyon et al. (2016) data cover basins throughout the US. All values are well-pad aggregates.

Figure A6: Measurements from Frankenberg et al. (2016)

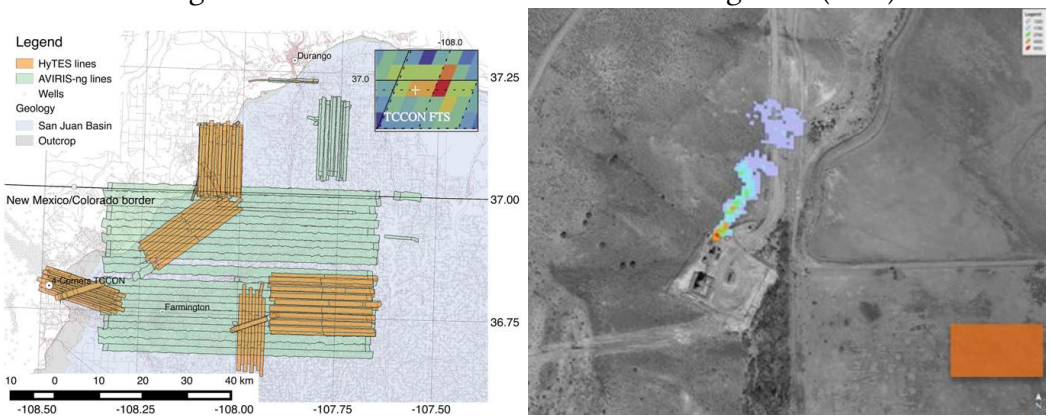

LEFT: Flight lines from Frankenberg et al. (2016). Only AVIRIS-NG flights, in green, were able to quantify emissions.
RIGHT: Gas storage tank, emitting ~146 kg CH_4 per hr, using AVIRIS-NG instrument. Orange bar is 60 m wide.

Figure A7: Natural gas prices

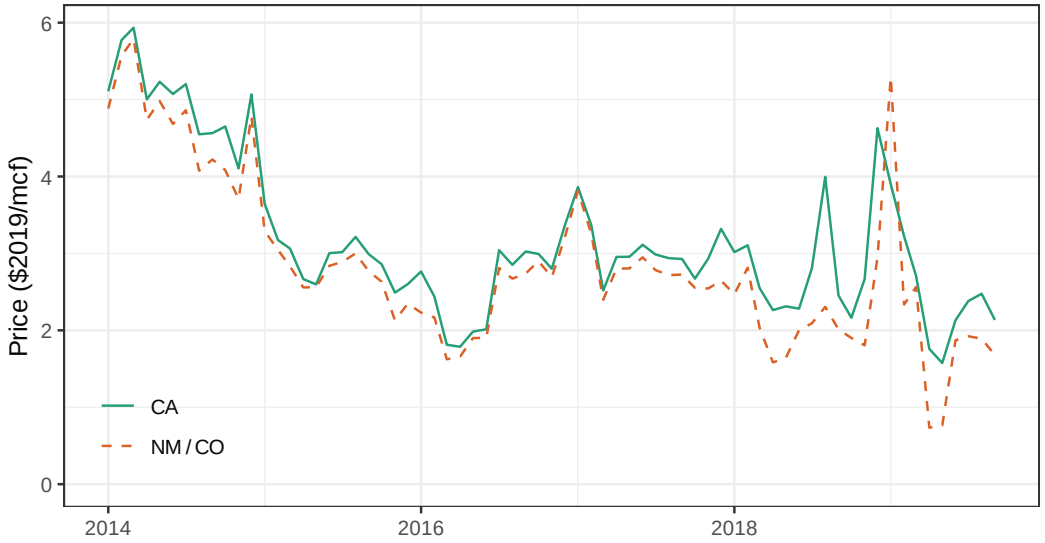

SOURCE: SNL Financial (SNL) natural gas price indexes for deliveries near study wells. We use the average of the SNL series "SoCal Gas" and "PG&E, South" for California wells and "El Paso, San Juan Basin" and "Transwestern, San Juan Basin" for the Four Corners wells. See text section 4.3 for details.

Figure A8: Matched natural gas prices exhibit little variation

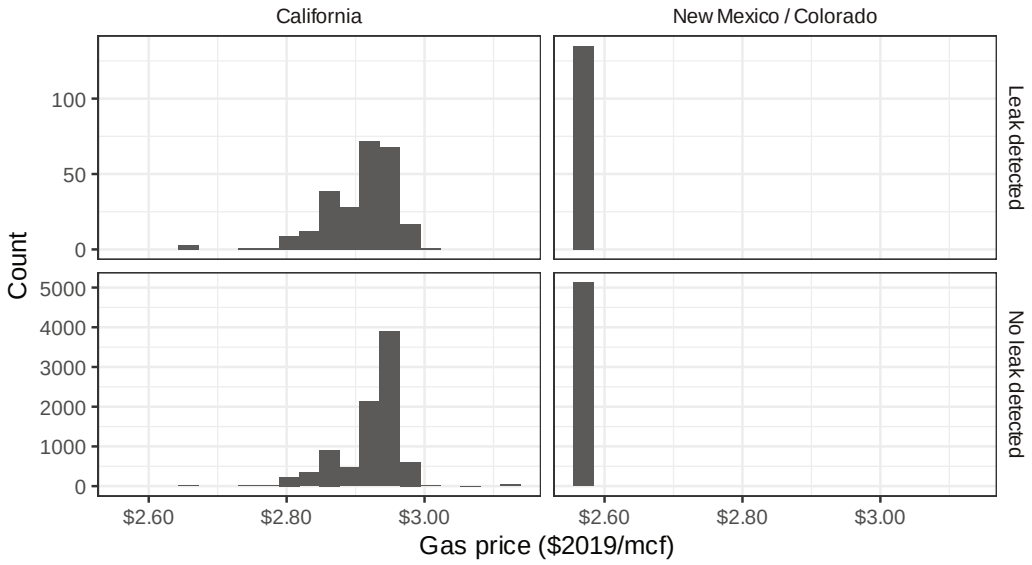

A3 Distribution Fitting

A3.1 Model Priors

We employ a fully Bayesian model, including priors on the parameters we estimate. As noted in the main text, we choose priors that are very weakly informative on the outcome scale. Specifically, we chose priors with mean zero and a standard deviation large enough that the predicted value of the outcomes e_i and q_i could take any reasonable value. For e_i, reasonable values are up to perhaps 100 times larger than the largest leak we see. For q_i, we aimed for a roughly uniform prior distribution by choosing priors of its underlying parameters. The prior standard deviations are much smaller here; because of the logit transformation, making the prior standard deviations larger would put a lot of prior weight on probabilities near zero or one (see Gelman et al. 2020 for much more discussion). We use a Student's t distribution with three degrees of freedom to allow for somewhat more weight in the distributions' tails than the Normal. Specifically, we de-mean all of the X variables and use priors of generalized Student's $t(3, 0, 3)$ for each of the leak size parameters β and σ. We use Normal$(0, 0.5)$ for the A_i coefficients (ψ) and Normal$(0, 0.75)$ for the α_i coefficients (ϕ). While these seem like fairly narrow priors on first glance, these values lead to diffuse priors of the A_i and α_i. After the inverse logit transformations described above, the priors on (ψ) and (ϕ) are compatible with a wide range of values of A_i and α_i. The prior covariance between coefficients are all zero.

A3.2 Estimated Parameters

Table A3: Estimated model parameters

	Leak size	Leak presence: ψ	Leak presence: ϕ
Intercept	4.99	−5.55	2.14
	[3.9,6.1]	[−6.8,−4.4]	[0.25,4.3]
IHS of age (yr)	0.0104	0.044	−0.228
	[−0.13,0.15]	[−0.12,0.21]	[−0.52,0.038]
IHS of gas prod (mcfd)	0.05	0.0916	−0.259
	[−0.077,0.18]	[−0.053,0.24]	[−0.44,−0.086]
IHS of oil prod (bbld)	−0.0115	0.114	0.424
	[−0.16,0.14]	[−0.056,0.29]	[0.03,0.9]
Basin: San Joaquin	−0.018	0.176	0.875
	[−0.58,0.54]	[−0.37,0.77]	[−0.13,1.8]
Basin: San Juan	−1.28	−0.336	0.0994
	[−2,−0.56]	[−1,0.34]	[−0.91,1]
Drill: Horizontal	0.476	0.00276	1.1
	[−0.37,1.3]	[−0.71,0.67]	[0.15,2.1]
Drill: Unknown	−0.265	0.224	−0.0705
	[−0.72,0.19]	[−0.76,1.2]	[−0.73,0.55]
Drill: Vertical	0.0494	0.355	1.53
	[−0.26,0.36]	[−0.038,0.78]	[0.88,2.2]
Oil prod share	0.0471	0.819	−0.515
	[−0.83,0.93]	[0.028,1.6]	[−1.9,0.76]
σ	0.998		
	[0.93,1.1]		
N	382	14058	
R^2	0.18	0.021	
Dep. var. mean	196	0.0271	

Note: Square brackets are 95% CI. Omitted category for drilling is directional. Omitted category for basin is all of California outside the San Joaquin basin.
Sources: See table 1.

Figure A9: Abatement elasticity ($-\hat{\alpha}_i$)

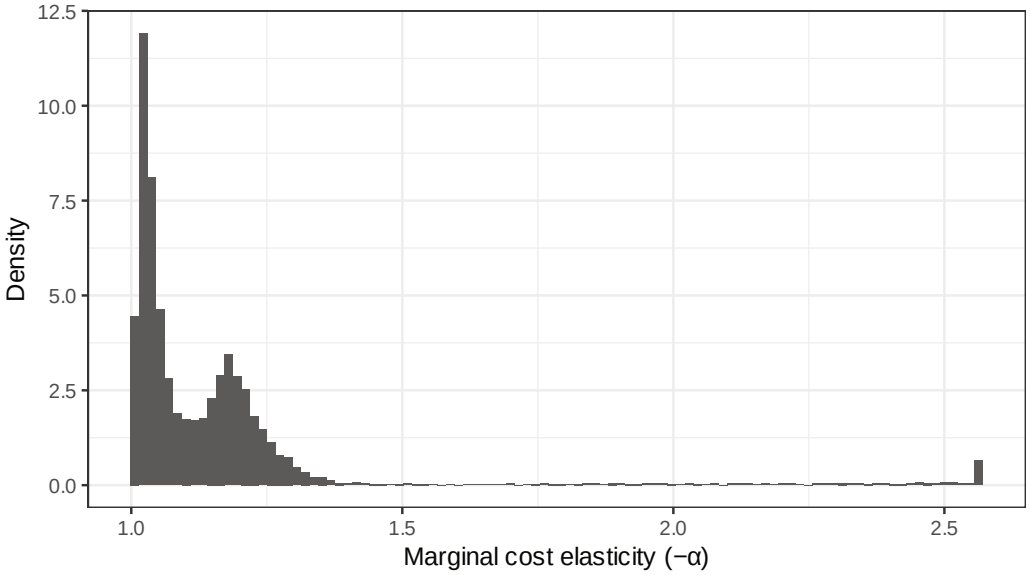

The plot shows the mean of Markov chain Monte Carlo (MCMC) draws of each well's α_i, from equation 3. Values are winsorized at the 99th percentile. See discussion in section 5.4.

A4 Alternative Presentations of Policy Simulation Output

This section provides tabular versions of figures 4 and 5. Please see those figures and the discussions in sections 6.1 and 6.2 for more description. In these tables, bracketed values indicate 95% confidence interval (CI).

Table A4: Expected fee, as a percentage of δ

	Mean (%)	Median (%)	p25 (%)	p75 (%)
τ = \$5 per ton CO_2e, T = 1 week				
Uniform	0.00143 [0.0014,0.0014]	0.00143 [0.0014,0.0014]	0.00143 [0.0014,0.0014]	0.00143 [0.0014,0.0014]
Target covariates	0.00143 [0.0014,0.0014]	0 [0,0]	0 [0,0]	0 [0,0]
Target leaks, high threshold	0.0512 [0.045,0.059]	0 [0,0]	0 [0,0]	0.143 [0.14,0.14]
Remote, high threshold	0.0819	0.143	0	0.143

	[0.08,0.087]	[0.14,0.14]	[0,0]	[0.14,0.14]
Target leaks, low threshold	0.05	0	0	0.143
	[0.046,0.059]	[0,0]	[0,0]	[0.14,0.14]
Remote, low threshold	0.143	0.143	0.143	0.143
	[0.14,0.14]	[0.14,0.14]	[0.14,0.14]	[0.14,0.14]
τ = \$5 per ton CO_2e, T = 3 months				
Uniform	0.0186	0.0186	0.0186	0.0186
	[0.019,0.019]	[0.019,0.019]	[0.019,0.019]	[0.019,0.019]
Target covariates	0.0186	0	0	0
	[0.019,0.019]	[0,0]	[0,0]	[0,0]
Target leaks, high threshold	0.832	0.101	0	1.86
	[0.72,0.96]	[0,1.9]	[0,0]	[1.9,1.9]
Remote, high threshold	1.07	1.86	0	1.86
	[1,1.1]	[1.9,1.9]	[0,0]	[1.9,1.9]
Target leaks, low threshold	0.806	0.0428	0	1.86
	[0.71,0.92]	[0,0.79]	[0,0]	[1.9,1.9]
Remote, low threshold	1.86	1.86	1.86	1.86
	[1.9,1.9]	[1.9,1.9]	[1.9,1.9]	[1.9,1.9]
$\tau = \delta$, T = 1 week				
Uniform	0.0192	0.0192	0.0192	0.0192
	[0.019,0.019]	[0.019,0.019]	[0.019,0.019]	[0.019,0.019]
Target covariates	0.0192	0	0	0
	[0.019,0.019]	[0,0]	[0,0]	[0,0]
Target leaks, high threshold	0.86	0.114	0	1.92
	[0.74,1]	[0,1.9]	[0,0]	[1.9,1.9]
Remote, high threshold	1.1	1.92	0	1.92
	[1.1,1.2]	[1.9,1.9]	[0,0]	[1.9,1.9]
Target leaks, low threshold	0.835	0.0494	0	1.92
	[0.73,0.96]	[0,0.93]	[0,0]	[1.9,1.9]
Remote, low threshold	1.92	1.92	1.92	1.92
	[1.9,1.9]	[1.9,1.9]	[1.9,1.9]	[1.9,1.9]
$\tau = 2\delta$, T = 1 week				
Uniform	0.0384	0.0384	0.0384	0.0384
	[0.038,0.038]	[0.038,0.038]	[0.038,0.038]	[0.038,0.038]
Target covariates	0.0384	0	0	0
	[0.038,0.038]	[0,0]	[0,0]	[0,0]

Target leaks, high threshold	2.09 [1.8,2.3]	3.11 [0,3.8]	0 [0,0]	3.84 [3.8,3.8]
Remote, high threshold	2.2 [2.1,2.3]	3.84 [3.8,3.8]	0 [0,0]	3.84 [3.8,3.8]
Target leaks, low threshold	2.04 [1.7,2.3]	2.84 [0.22,3.8]	0 [0,0]	3.84 [3.8,3.8]
Remote, low threshold	3.84 [3.8,3.8]	3.84 [3.8,3.8]	3.84 [3.8,3.8]	3.84 [3.8,3.8]
$\tau = \delta$, $T = 3$ months				
Uniform	0.25 [0.25,0.25]	0.25 [0.25,0.25]	0.25 [0.25,0.25]	0.25 [0.25,0.25]
Target covariates	0.25 [0.25,0.25]	0 [0,0]	0 [0,0]	0.00295 [0,0.071]
Target leaks, high threshold	14.4 [14,15]	25 [25,25]	0 [0,0]	25 [25,25]
Remote, high threshold	14.3 [14,15]	25 [25,25]	0 [0,0]	25 [25,25]
Target leaks, low threshold	25 [25,25]	25 [25,25]	25 [25,25]	25 [25,25]
Remote, low threshold	25 [25,25]	25 [25,25]	25 [25,25]	25 [25,25]
$\tau = 2\delta$, $T = 3$ months				
Uniform	0.5 [0.5,0.5]	0.5 [0.5,0.5]	0.5 [0.5,0.5]	0.5 [0.5,0.5]
Target covariates	0.5 [0.5,0.5]	0 [0,0]	0 [0,0]	0.299 [0,0.66]
Target leaks, high threshold	28.8 [28,31]	50 [50,50]	0 [0,0]	50 [50,50]
Remote, high threshold	28.6 [28,30]	50 [50,50]	0 [0,0]	50 [50,50]
Target leaks, low threshold	50 [50,50]	50 [50,50]	50 [50,50]	50 [50,50]
Remote, low threshold	50 [50,50]	50 [50,50]	50 [50,50]	50 [50,50]

Table A5: Reduction in DWL and Emissions

	DWL reduction(%)	Emiss. reduction (%)
τ = \$5 per ton CO_2e, T = 1 week		
Uniform	0.0153	0.0196
	[0.014,0.016]	[0.019,0.02]
Target covariates	0.0945	0.087
	[0.06,0.13]	[0.058,0.11]
Target leaks, high threshold	1.27	1.09
	[1.1,1.3]	[0.97,1.1]
Remote, high threshold	1.64	1.39
	[1.6,1.7]	[1.3,1.4]
Target leaks, low threshold	1.3	1.11
	[1.2,1.4]	[0.99,1.2]
Remote, low threshold	2.26	1.92
	[2.2,2.3]	[1.9,2]
τ = \$5 per ton CO_2e, T = 3 months		
Uniform	0.291	0.254
	[0.29,0.3]	[0.25,0.26]
Target covariates	1.11	0.956
	[0.76,1.4]	[0.66,1.2]
Target leaks, high threshold	15.6	13.4
	[14,16]	[12,14]
Remote, high threshold	17.3	14.8
	[17,18]	[14,15]
Target leaks, low threshold	16.3	14
	[14,17]	[12,15]
Remote, low threshold	23.9	20.5
	[24,24]	[20,21]

$\tau = \delta$, $T = 1$ week		
Uniform	0.3	0.262
	[0.3,0.31]	[0.26,0.27]
Target covariates	1.14	0.98
	[0.78,1.5]	[0.68,1.3]
Target leaks, high threshold	16	13.8
	[15,17]	[12,14]
Remote, high threshold	17.7	15.2
	[17,18]	[15,15]
Target leaks, low threshold	16.8	14.4
	[15,18]	[13,15]
Remote, low threshold	24.4	21
	[24,25]	[21,21]
$\tau = 2\delta$, $T = 1$ week		
Uniform	0.606	0.522
	[0.6,0.62]	[0.52,0.54]
Target covariates	2.01	1.73
	[1.4,2.6]	[1.2,2.2]
Target leaks, high threshold	28.6	24.8
	[27,29]	[24,25]
Remote, high threshold	29.3	25.3
	[28,30]	[25,26]
Target leaks, low threshold	32	27.7
	[29,34]	[25,29]
Remote, low threshold	40.4	34.9
	[40,41]	[35,36]
$\tau = \delta$, $T = 3$ months		

Uniform	3.88	3.31
	[3.8,4]	[3.3,3.4]
Target covariates	8.24	7.11
	[6.7,9.7]	[5.8,8.4]
Target leaks, high threshold	65.2	59.6
	[63,66]	[58,60]
Remote, high threshold	64.2	58.7
	[62,65]	[57,60]
Target leaks, low threshold	88.6	80.9
	[88,89]	[81,82]
Remote, low threshold	88.6	80.9
	[88,89]	[81,82]
$\tau = 2\delta$, $T = 3$ months		
Uniform	7.52	6.42
	[7.4,7.7]	[6.3,6.6]
Target covariates	13.7	11.8
	[12,15]	[10,13]
Target leaks, high threshold	72.8	69
	[71,74]	[67,70]
Remote, high threshold	70.5	67
	[68,72]	[65,68]
Target leaks, low threshold	97.4	92.5
	[97,98]	[92,93]
Remote, low threshold	97.4	92.5
	[97,98]	[92,93]

Figure A10: Curvature of DWL and Emission Outcomes

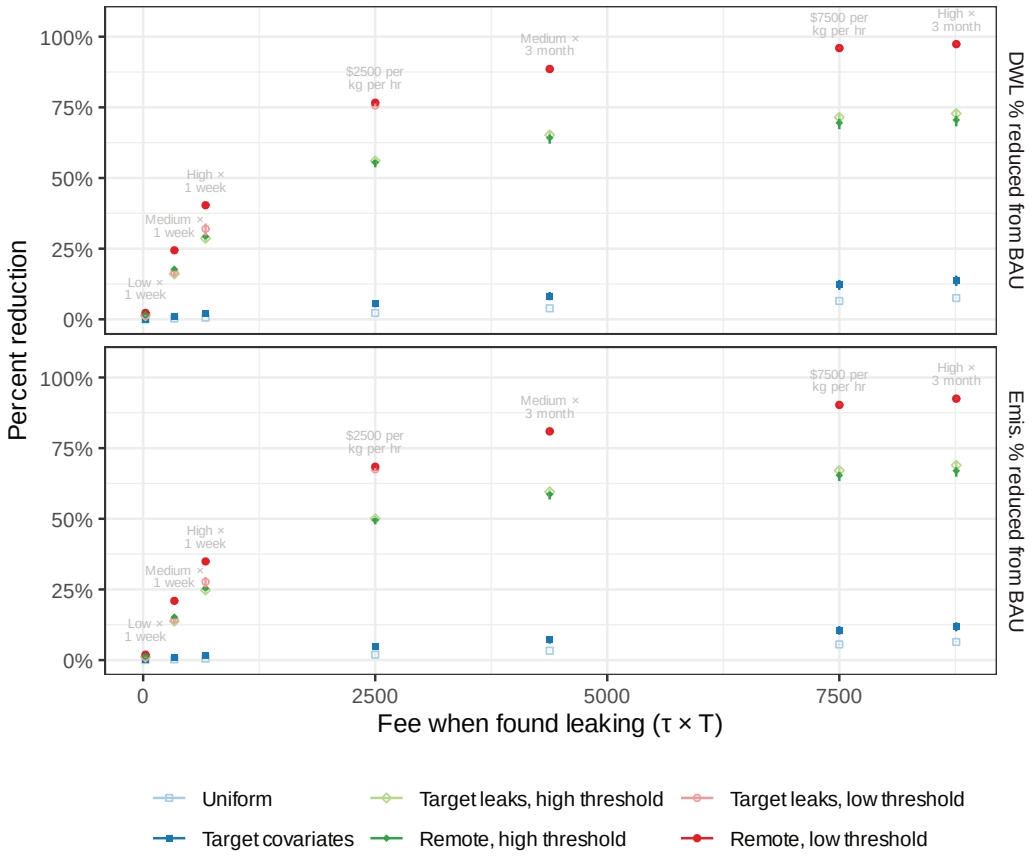

This graph presents a version of the main-text figure 5, with x-axis values plotted on a cardinal scale, allowing the reader to have a better sense of the curvature of the DWL and emissions outcomes at different fee levels. This plot excludes the case of $\tau \times T = \text{low} \times 3$ months for better visualization, as this case is fairly close to $\tau \times T = \text{med} \times 1$ week. The plot includes two additional x-axis values, at $\tau \times T = 2500$ and 7500, chosen to improve coverage over the x-axis domain. We present these additional points, rather than a smoother curve, because the computing required for each x-axis value is time-consuming.

A5 Drilling Response Details

The main text considered the abatement behavior in a fixed population of wells. However, charging additional fees and increasing abatement costs will make it less profitable to operate a well, and in equilibrium we expect the number of new wells drilled to decline. This effect ends up being small relative to the per-well abatement.

First, we convert our methane leak fees into their approximate equivalent reduction in well profit from a change in prices. Briefly, we total the well's expected fee payments and abatement costs, and find the change in commodity price that would result in an equivalent change to well profit, assuming the production quantity is unchanged. Once we've calculated this price-equivalent change, we borrow supply and demand elasticities from the literature to estimate the change in drilling. Both the profit-equivalent price change (11.8%) and the elasticity of drilling (0.36) are small, so this margin does not substantially affect our conclusions.

This calculation requires stronger assumptions than we applied in the main text. We consider the extensive margin: wells that face some fee for their emissions will see lower profits, all else equal, than wells that face no fees. Therefore, fewer wells will be drilled. It is unlikely that existing wells will stop producing, or that wells will change the amount they produce (Anderson, Kellogg, and Salant 2018). To keep things simple, we assume that there's no change in the composition of wells drilled.

To estimate an approximate drilling response, we first translate our expected fees into profit-equivalent changes in the price of natural gas, then we use estimates from the literature of the elasticity of drilling with respect to price. Further, we assume that a well's cost of drilling does not change in this scenario, except for the cost of abatement. We also assume that the policy does not lead to any change in the commodity price of natural gas.

To define some notation, say that without any methane policy a well operator spends D to drill a well, and implement the privately optimal level of abatement. They earn Ep_0 revenue on the well's operation. Here we elide complications like

prices changing over time, uncertainty, and discounting.[1] With under an audit policy, they still spend D to drill the well, but now they also spend an additional C on abatement and F on expected fees. Revenue is now $(E+\epsilon)p_0$, since some additional gas may be captured. We define the profit-equivalent price change as the (lower) price that would result in the same profit the well would earn under the no-policy case. The profit-equivalent price change is:

$$\Delta p = \frac{C + F - \epsilon p_0}{E}$$

For this calculation, we consider considering (3b), which uses remote measurements to target leaks and a realistic detection threshold. Using the highest fee we considered ($\tau = 2\delta$ and T = 3 months), we find the production-weighted average price-equivalent is 11.8% of the wholesale prices in our sample (which are approx. $2.90–3.90).

For the price elasticity of drilling we rely on Gilbert and Roberts (2020), which calculates that the production-weighted long run elasticity of gas drilling with respect to the Henry Hub gas price is about 0.36 for all onshore drilling in the continental US, or 0.93 for their five-basin focus. [2]

Combining these, we come to the conclusion presented in the main text. Even a high-fee policy would see at most a 5–10% reduction in new (production weighted) drilling, and therefore the changes in expected emissions from this margin are small.

A6 Robustness to Alternative Sets of Variables

As a robustness check of our specification, we run our analysis for the fee scenario of $\tau \times T = \delta \times 3$ months using all subsets of our preferred set with at least two

[1] Here we rely on a martingale price assumption, that today's price is the best guess for tomorrow's price. Ignoring discounting is less of a problem than it would seem because we consider a change in price that applies to every future period, just as the expected change in profits applies in every future period.

[2] In table 6 of that paper, the authors report the continental US short-run elasticity of 0.17 (s.e. 0.096), with the coefficient on the lagged dependent variable of 0.53 (s.e. 0.96). We calculate the approximate long-run elasticity as 0.36 (= 0.17 / (1 − 0.53)).

variables (56 specifications), plus combinations that use sub-basin fixed effects and inverse hyperbolic sine number of wells within 10 km (3 specifications [3]).

The sub-basin fixed effects are modeled by density-based spatial clustering of applications with noise (DBSCAN), an unsupervised learning technique that assigns well pads to clusters and outliers. DBSCAN works by identifying clusters as regions of high density that are separated by regions of low density. In contrast to counting the number of wells within a fixed radius, DBSCAN can handle irregular geographic distributions of wells. We used geospatial coordinates to cluster, and selected DBSCAN parameters to provide subjectively reasonable-looking cluster patterns. We end up with four clusters in the densely drilled San Joaquin basin, six in the rest of California, and one large cluster in the San Juan basin. When we use these fixed effects in the regressions, we include one fixed effect level per cluster, and one level for each basin's outliers. By including the sub-basin fixed effects and/or the number of wells within 10 km, our aim is to control for the well density information that was not accounted for in our preferred specification.

In figure A11, the preferred specification is in black and the other specifications are in gray. The points for the preferred specification are qualitatively similar to the others. There are a few features to note here. The range across specifications is quite narrow: roughly 10 percentage points from the lowest to the highest. The confidence intervals here overlap substantially. From these features, we conclude that our takeaways do not depend dramatically on the particular specification choice, at least among the variables included.

[3](1) our main specification with basin dummies replaced by sub-basin cluster dummies, (2) our main specification plus the number of wells within 10 km, and (3) both.

Figure A11: Comparison across specifications

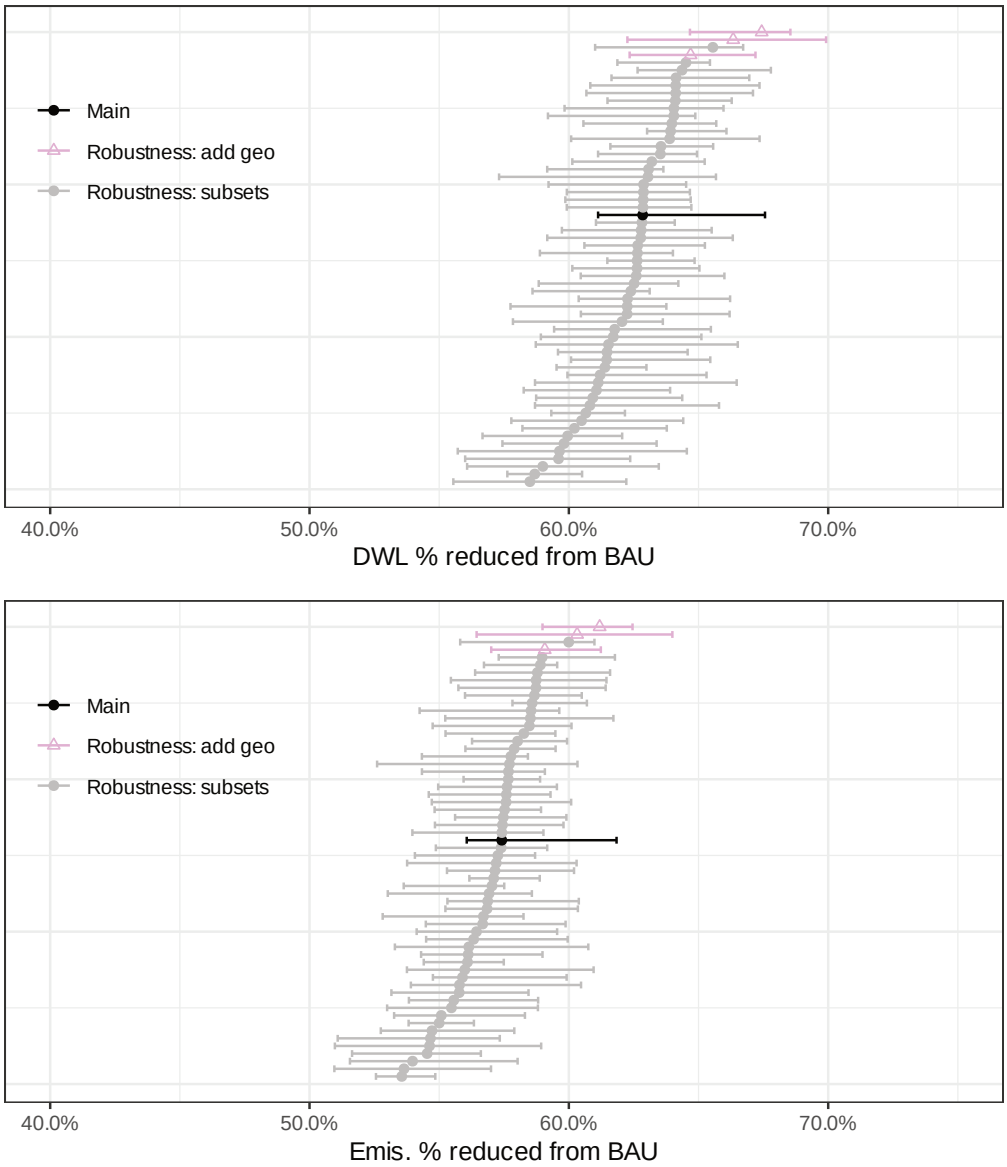

The top and bottom panels plot the change in DWL and emissions for the case of $\tau \times T = \delta \times 3$ months. The black point is our preferred specification (see variables in table A3). The gray and pink points are alternative specifications, using subsets of the main specification and additional geographic variables. These specifications are described in in appendix section A6. Bars indicate 95% CI. To save computation resources, both the estimates and the confidence intervals are derived from standard MCMC values, as opposed to the more computationally intensive Bayes-Bag procedure employed in the main results of the paper. These non-bootstrapped CIs are qualitatively similar to, and are slightly larger than, the bootstrapped CIs reported in figure 5.

References

Alvarez, Ramón A, Daniel Zavala-Araiza, David R Lyon, David T Allen, Zachary R Barkley, Adam R Brandt, Kenneth J Davis, et al. 2018. "Assessment of methane emissions from the U.S. oil and gas supply chain." *Science* (June): eaar7204. https://doi.org/10.1126/science.aar7204.

Anderson, Soren T, Ryan Kellogg, and Stephen W Salant. 2018. "Hotelling under Pressure." *Journal of Political Economy* 126, no. 3 (June): 984–1026. https://doi.org/10.1086/697203.

Cusworth, Daniel H, Daniel J Jacob, Daniel J Varon, Christopher Chan Miller, Xiong Liu, Kelly Chance, Andrew K Thorpe, et al. 2019. "Potential of next-generation imaging spectrometers to detect and quantify methane point sources from space." *Atmospheric Measurement Techniques* 12, no. 10 (October): 5655–5668. https://doi.org/10.5194/amt-12-5655-2019.

Duren, Riley M, Andrew K Thorpe, Kelsey T Foster, Talha Rafiq, Francesca M Hopkins, Vineet Yadav, Brian D Bue, et al. 2019. "California's methane super-emitters." *Nature* 575, no. 7781 (November): 180–184. https://doi.org/10.1038/s41586-019-1720-3.

Frankenberg, Christian, Andrew K Thorpe, David R Thompson, Glynn Hulley, Eric Adam Kort, Nick Vance, Jakob Borchardt, et al. 2016. "Airborne methane remote measurements reveal heavy-tail flux distribution in Four Corners region." *Proceedings of the National Academy of Sciences* 113, no. 35 (August): 9734–9739. https://doi.org/10.1073/pnas.1605617113.

Gelman, Andrew, Aki Vehtari, Daniel Simpson, Charles C Margossian, Bob Carpenter, Yuling Yao, Lauren Kennedy, Jonah Gabry, Paul-Christian Bürkner, and Martin Modrák. 2020. "Bayesian Workflow" (November 3, 2020). arXiv: 2011.01808 [stat.ME].

Gilbert, Ben, and Gavin Roberts. 2020. "Drill-Bit Parity: Supply-Side Links in Oil and Gas Markets." *Journal of the Association of Environmental and Resource Economists* 7, no. 4 (July): 619–658. https://doi.org/10.1086/708160.

Hester, Jim, and Jennifer Bryan. 2022. *glue: Interpreted String Literals.* 1.6.2. https://CRAN.R-project.org/package=glue.

Lyon, David R, Ramón A Alvarez, Daniel Zavala-Araiza, Adam R Brandt, Robert B Jackson, and Steven P Hamburg. 2016. "Aerial Surveys of Elevated Hydrocarbon Emissions from Oil and Gas Production Sites." *Environmental Science & Technology* 50, no. 9 (April): 4877–4886. https://doi.org/10.1021/acs.est.6b00705.

Marks, Levi. 2022. "The Abatement Cost of Methane Emissions from Natural Gas Production." *Journal of the Association of Environmental and Resource Economists* (January 5, 2022). https://doi.org/10.1086/716700.

Omara, Mark, Melissa R Sullivan, Xiang Li, R Subramanian, Allen L Robinson, and Albert A Presto. 2016. "Methane Emissions from Conventional and Unconventional Natural Gas Production Sites in the Marcellus Shale Basin." *Environmental Science & Technology* 50, no. 4 (November): 2099–2107. https://doi.org/10.1021/acs.est.5b05503.

Omara, Mark, Naomi Zimmerman, Melissa R Sullivan, Xiang Li, Aja Ellis, Rebecca Cesa, R Subramanian, Albert A Presto, and Allen L Robinson. 2018. "Methane Emissions from Natural Gas Production Sites in the United States: Data Synthesis and National Estimate." *Environmental Science & Technology* 52, no. 21 (September): 12915–12925. https://doi.org/10.1021/acs.est.8b03535.

Rella, Chris W, Tracy R Tsai, Connor G Botkin, Eric R Crosson, and David Steele. 2015. "Measuring Emissions from Oil and Natural Gas Well Pads Using the Mobile Flux Plane Technique." *Environmental Science & Technology* 49, no. 7 (March): 4742–4748. https://doi.org/10.1021/acs.est.5b00099.

Robertson, Anna M, Rachel Edie, Dustin Snare, Jeffrey Soltis, Robert A Field, Matthew D Burkhart, Clay S Bell, Daniel Zimmerle, and Shane M Murphy. 2017. "Variation in Methane Emission Rates from Well Pads in Four Oil and Gas Basins with Contrasting Production Volumes and Compositions." *Environmental Science & Technology* 51, no. 15 (July): 8832–8840. https://doi.org/10.1021/acs.est.7b00571.

Software Citations

Bache, Stefan Milton, and Hadley Wickham. 2020. *magrittr: A Forward-Pipe Operator for R.* 2.0.1. https://CRAN.R-project.org/package=magrittr.

Bengtsson, Henrik. 2020. *A Unifying Framework for Parallel and Distributed Processing in R using Futures,* August. arXiv: 2008.00553 [cs.DC]. https://arxiv.org/abs/2008.00553.

———. 2021. *matrixStats: Functions that Apply to Rows and Columns of Matrices (and to Vectors).* 0.60.0. https://CRAN.R-project.org/package=matrixStats.

Bürkner, Paul-Christian, Jonah Gabry, Matthew Kay, and Aki Vehtari. 2023. *posterior: Tools for Working with Posterior Distributions.* 1.4.1. https://mc-stan.org/posterior/.

Csárdi, Gábor, and Winston Chang. 2021. *processx: Execute and Control System Processes.* 3.5.2. https://CRAN.R-project.org/package=processx.

Csárdi, Gábor, Jim Hester, Hadley Wickham, Winston Chang, Martin Morgan, and Dan Tenenbaum. 2021. *remotes: R Package Installation from Remote Repositories, Including 'GitHub'.* 2.4.2. https://CRAN.R-project.org/package=remotes.

Csardi, Gabor, and Tamas Nepusz. 2006. "The igraph software package for complex network research." *InterJournal* Complex Systems:1695. https://igraph.org.

Dorman, Michael. 2021. *nngeo: k-Nearest Neighbor Join for Spatial Data.* 0.4.3. https://CRAN.R-project.org/package=nngeo.

Dowle, Matt, and Arun Srinivasan. 2021. *data.table: Extension of 'data.frame'.* 1.14.0. https://CRAN.R-project.org/package=data.table.

Fabri, Antoine. 2022. *powerjoin: Extensions of 'dplyr' and 'fuzzyjoin' Join Functions.* 0.1.0. https://CRAN.R-project.org/package=powerjoin.

FC, Mike, Trevor L Davis, and ggplot2 authors. 2022. *ggpattern: 'ggplot2' Pattern Geoms.* 1.0.0. https://CRAN.R-project.org/package=ggpattern.

Gabry, Jonah, and Rok Češnovar. 2022. *cmdstanr: R Interface to 'CmdStan'.* https://mc-stan.org/cmdstanr/.

Grolemund, Garrett, and Hadley Wickham. 2011. "Dates and Times Made Easy with lubridate." *Journal of Statistical Software* 40 (3): 1–25. https://www.jstatsoft.org/v40/i03/.

Henry, Lionel, and Hadley Wickham. 2023. *rlang: Functions for Base Types and Core R and 'Tidyverse' Features.* 1.1.0. https://CRAN.R-project.org/package=rlang.

———. 2021. *tidyselect: Select from a Set of Strings.* 1.1.1. https://CRAN.R-project.org/package=tidyselect.

Hester, Jim, and Hadley Wickham. 2020. *fs: Cross-Platform File System Operations Based on 'libuv'.* 1.5.0. https://CRAN.R-project.org/package=fs.

Iannone, Richard, Joe Cheng, and Barret Schloerke. 2021. *gt: Easily Create Presentation-Ready Display Tables.* 0.3.0. https://CRAN.R-project.org/package=gt.

Köster, Johannes, and Sven Rahmann. 2018. "Snakemake—a scalable bioinformatics workflow engine." *Bioinformatics* 34, no. 20 (May): 3600–3600. https://doi.org/10.1093/bioinformatics/bty350.

Langa, Łukasz, et al. 2020. *Black: The uncompromising code formatter.* https://black.readthedocs.io.

McKinney, Wes, et al. 2010. "Data structures for statistical computing in python." In *Proceedings of the 9th Python in Science Conference,* 445:51–56. Austin, TX.

Müller, Kirill. 2020. *here: A Simpler Way to Find Your Files.* 1.0.1. https://CRAN.R-project.org/package=here.

Müller, Kirill, and Hadley Wickham. 2021. *tibble: Simple Data Frames.* 3.1.3. https://CRAN.R-project.org/package=tibble.

Neuwirth, Erich. 2014. *RColorBrewer: ColorBrewer Palettes.* 1.1-2. https://CRAN.R-project.org/package=RColorBrewer.

Ooms, Jeroen. 2021. *curl: A Modern and Flexible Web Client for R.* 4.3.2. https://CRAN.R-project.org/package=curl.

———. 2014. "The jsonlite Package: A Practical and Consistent Mapping Between JSON Data and R Objects." *arXiv:1403.2805 [stat.CO],* https://arxiv.org/abs/1403.2805.

———. 2020. *unix: POSIX System Utilities.* 1.5.2. https://CRAN.R-project.org/package=unix.

Pebesma, Edzer. 2018. "Simple Features for R: Standardized Support for Spatial Vector Data." *The R Journal* 10 (1): 439–446. https://doi.org/10.32614/RJ-2018-009. https://doi.org/10.32614/RJ-2018-009.

Pebesma, Edzer, Thomas Mailund, and James Hiebert. 2016. "Measurement Units in R." *R Journal* 8 (2): 486–494. https://doi.org/10.32614/RJ-2016-061.

Pedregosa, F., G. Varoquaux, A. Gramfort, V. Michel, B. Thirion, O. Grisel, M. Blondel, et al. 2011. "Scikit-learn: Machine Learning in Python." *Journal of Machine Learning Research* 12:2825–2830.

R Core Team. 2022. *R: A Language and Environment for Statistical Computing.* Vienna, Austria: R Foundation for Statistical Computing. https://www.R-project.org/.

Richardson, Neal, Ian Cook, Nic Crane, Jonathan Keane, Romain François, Jeroen Ooms, and Apache Arrow. n.d. *arrow: Integration to 'Apache' 'Arrow'.* https://arrow.apache.org/docs/r/.

Stan Development Team. 2023. *CmdStan: The Shell Interface to Stan.* 2.32.2. May 15, 2023. https://mc-stan.org/users/interfaces/cmdstan.

Van Rossum, Guido, and Fred L. Drake. 2009. *Python 3 Reference Manual.* Scotts Valley, CA: CreateSpace.

Vaughan, Davis, and Matt Dancho. 2021. *furrr: Apply Mapping Functions in Parallel using Futures.* 0.2.3. https://CRAN.R-project.org/package=furrr.

Virtanen, Pauli, Ralf Gommers, Travis E. Oliphant, Matt Haberland, Tyler Reddy, David Cournapeau, Evgeni Burovski, et al. 2020. "SciPy 1.0: Fundamental Algorithms for Scientific Computing in Python." *Nature Methods* 17:261–272. https://doi.org/10.1038/s41592-019-0686-2.

Wächter, Andreas, and Lorenz T. Biegler. 2005. "On the implementation of an interior-point filter line-search algorithm for large-scale nonlinear programming." *Mathematical Programming* 106, no. 1 (April 28, 2005): 25–57. https://doi.org/10.1007/s10107-004-0559-y.

Walt, Stéfan van der, S Chris Colbert, and Gaël Varoquaux. 2011. "The NumPy Array: A Structure for Efficient Numerical Computation." *Computing in Science & Engineering* 13, no. 2 (March): 22–30. https://doi.org/10.1109/mcse.2011.37.

Wickham, Hadley. 2016. *ggplot2: Elegant Graphics for Data Analysis.* Springer-Verlag New York. https://ggplot2.tidyverse.org.

———. 2019. *stringr: Simple, Consistent Wrappers for Common String Operations.* 1.4.0. https://CRAN.R-project.org/package=stringr.

———. 2021. *tidyr: Tidy Messy Data.* 1.1.3. https://CRAN.R-project.org/package=tidyr.

Wickham, Hadley, and Jennifer Bryan. 2019. *readxl: Read Excel Files.* 1.3.1. https://CRAN.R-project.org/package=readxl.

Wickham, Hadley, Romain François, Lionel Henry, and Kirill Müller. 2021. *dplyr: A Grammar of Data Manipulation.* 1.0.7. https://CRAN.R-project.org/package=dplyr.

Wickham, Hadley, and Lionel Henry. 2022. *purrr: Functional Programming Tools.* 1.0.0. https://CRAN.R-project.org/package=purrr.

Wickham, Hadley, Jim Hester, and Jeroen Ooms. 2020. *xml2: Parse XML.* 1.3.2. https://CRAN.R-project.org/package=xml2.